volume-surface integral equations using higher-order hierarchical Legendre basis functions, Radio Sci 42 (2007), RS4023.
16. COMSOL Multiphysics 3.4, COMSOL Inc., available at: www.comsol.com.
17. E. Jørgensen, O.S. Kim, P. Meincke, and O. Breinbjerg, Higher order hierarchical Legendre basis functions in integral equation formulations applied to complex electromagnetic problems, In: Proceedings of IEEE AP-S International Symposium, Washington, DC, 3–8 July, Vol. 3A, 2005, pp. 64–67.
18. E. Jørgensen, J.L. Volakis, P. Meincke, and O. Breinbjerg, Higher order hierarchical Legendre basis functions for electromagnetic modeling, IEEE Trans Antennas Propag 52 (2004), 2985–2995.
19. S.R. Best, Low Q electrically small linear and elliptically polarized spherical dipole antennas, Trans Antennas Propag 53 (2005), 1047–1053.
20. A.D. Yaghjian and S.R. Best, Impedance, bandwidth, and Q of antennas, IEEE Trans Antennas Propag 53 (2005), 1298–1324.

ULTRA-WIDEBAND SLOT ANTENNA WITH BAND-NOTCH CHARACTERISTICS FOR WIRELESS USB DONGLE APPLICATIONS

Deepti Das Krishna, M. Gopikrishna, C. K. Aanandan, P. Mohanan, and K. Vasudevan
Centre for Research in Electromagnetics and Antennas, Department of Electronics, Cochin University of Science & Technology, Cochin 682022, India; Corresponding author: anand@cusat.ac.in

Received 17 September 2008

ABSTRACT: *A compact ultra-wideband (UWB) printed slot antenna is described, suitable for integration with the printed circuit board (PCB) of a wireless, universal, serial-bus dongle. The design comprises of a near-rectangular slot fed by a coplanar waveguide (CPW) printed on a PCB of size 20 × 30 mm². It has a large bandwidth covering the 3.1–10.6 GHz UWB band, with omnidirectional radiation patterns. Further, a notched band centered at 5.45 GHz wireless local area network bands is obtained within the wide bandwidth by inserting a narrow slot inside the tuning stub. Details of the antenna design are described, and the experimental results of the constructed prototype are presented. The time domain studies on the antenna shows a linear phase response throughout the band except at the notched frequency. The transient analysis of the antenna indicates very little pulse distortion confirming its suitability for high speed wireless connectivity.* © 2009 Wiley Periodicals, Inc. Microwave Opt Technol Lett 51: 1500–1504, 2009; Published online in Wiley InterScience (www.interscience.wiley.com). DOI 10.1002/mop.24385

Key words: *universal serial-bus (USB) dongle antennas; frequency notched antennas; CPW-fed antenna; ultra-wideband (UWB) antenna*

1. INTRODUCTION

Ultra-wideband (UWB) radios operating at high frequencies make possible data rates comparable with the fastest USB interconnects. Wireless USB (WUSB) combines the benefits of USB with the convenience of wireless technology leading to data rates up to 480 Mbps at 3 ms and up to 110 Mbps at 10 ms [1]. WUSB is one of the most promising applications of UWB technology and among the first to be commercially available for short-range and high-speed wireless interfaces. WUSB dongles replace USB cables and deliver instant UWB connectivity for a wide range of devices such as printers, hubs, and external hard drives. The dongles use an on-board UWB antenna on a printed circuit board (PCB) typically of 23 × 70 mm² size. Along with miniaturized size and omnidirectional radiation patterns, dongle antennas should be flexible in design with ground independence [2]. A microstrip-fed monopole antenna with reduced ground plane effects and a bended plate monopole antenna are reported for WUSB dongle applications in [3] and [4], respectively.

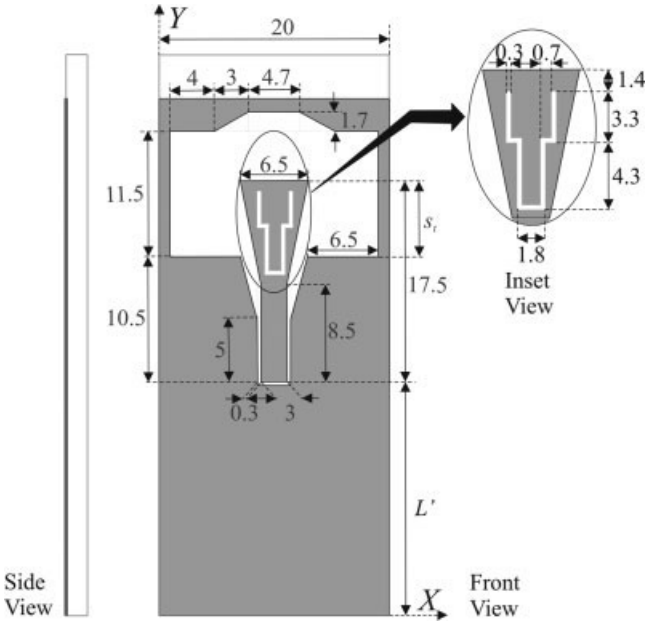

Figure 1 The proposed slot antenna

After the FCC allocation of 3.1–10.6 GHz frequency band for commercial applications, there has been considerable interest in the development of planar UWB antennas [5]. Planar wide slot antenna, with bidirectional radiation patterns and medium gain, is one of the most attractive candidates for UWB operation [6–11]. Wide slots of various geometrical shapes like circular/elliptical [6–8], rectangular [9], inverted cone [10], Koch Fractal [11], excited by fork-like [6, 11], circular [7, 8], rectangular [9] or inverted cone-shaped [10] tuning stubs, and fed by either microstrip line or coplanar waveguide (CPW) has been designed for ultrawideband operation. The proposed antenna uses a near-rectangular slot which along with a tapered tuning stub exhibits a wide impedance bandwidth from 2.9 to 11 GHz. The effect of the PCB/ground length on the antenna is observed to be negligible and along with the fact that the width of the antenna is restricted to 20 mm, the proposed design is suitable as WUSB dongle antenna. A CPW-feed further ensures easy integration with the rest of the USB circuitry. The proposed antenna is successfully designed, built, and verified. The antenna has excellent impedance matching, stable radiation patterns, and linear group delay over the entire UWB band along with good impulse response. In this article, the antenna design is further extended to the band-notched function to minimize potential interferences with the existing bands used by wireless local area networks (WLANs). To reject the 5.15–5.825 GHz band (IEEE802.11a and HIPERLAN/2), a narrow half wavelength long slot is embedded in the tuning stub. The simulation studies on the antenna have been carried out using Ansoft HFSS [12].

2. ANTENNA DESIGN

Figure 1 shows the geometry of the proposed antenna. The antenna consists of a near-rectangular aperture etched out from the ground plane of a PCB and a CPW-fed tapered tuning stub. The CPW feed

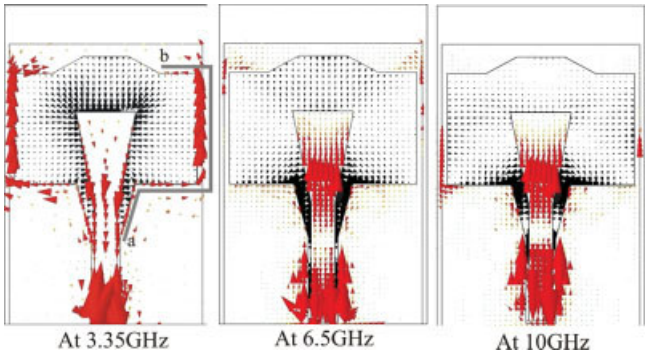

Figure 2 Current distribution and aperture electric field of the antenna at different resonant frequencies. [Color figure can be viewed in the online issue, which is available at www.interscience.wiley.com]

is designed for 50 Ω on FR4 substrate with $\varepsilon_r = 4.4$ and thickness $h = 1.6$ mm. Because the feed and the ground are implemented on the same plane, only one layer of substrate with single-sided metallization is used, making the antenna easy and cost-effective to manufacture. Simulated results indicate that the antenna resonates at three distinct frequencies, namely 3.35 GHz, 6.5 GHz, and 10 GHz, within the 3.1–10.6 GHz UWB band. The current distribution on the antenna plotted in Figure 2 indicates that the first resonance is due to the slot geometry because the longest current path is following the slot boundary. A half wavelength variation is observed along the slot boundary "*ab*" [shown in Fig. 2(a)] and is confirmed using Eq. (1).

$$\text{Slot length } \text{“}ab\text{”} = \frac{\lambda_{o1}}{2\sqrt{\varepsilon_{\text{eff}}}} \tag{1}$$

where $\varepsilon_{\text{eff}} = (\varepsilon_r + 1)/2$, and λ_{o1} is the free space wavelength at the first resonance.

The second resonance is due to the monopole like behavior of the tuning stub as in Eq. (2).

$$\text{Stub length } \text{“}s_t\text{”} = \frac{\lambda_{o1}}{4\sqrt{\varepsilon_{\text{eff}}}} \tag{2}$$

The third resonance is observed to be a higher order mode which is confirmed from the aperture field distribution also plotted in Figure 2. The strong *X*-field components on either sides of the stub cancel in the far field at all the resonances resulting in linear polarization along the *Y*-axis. A smooth transition from one antenna mode to another enables a wideband impedance matching. In this case, it is achieved by tapering the tuning stub and by modifying slot boundary near the feed and at the top of the tuning stub. A narrow slot embedded in the tuning stub is incorporated in the design to notch out the undesired WLAN frequencies in the 5.15–5.825 GHz band.

The overall size of the proposed UWB antenna is compact (20×30 mm^2) with its width comparable with practical, wireless USB dongles. However, while integrating the UWB antenna with the system ground plane of USB dongles, with lengths typically ranging at 70 mm, the antenna performance gets detuned as a result of using PCBs with various ground-plane lengths. Hence, to prove the suitability of the proposed design for WUSB applications, the effect of the ground plane length on the antenna is studied. Figure 3 plots the VSWR of the antenna for different ground lengths (L') and it shows that there is negligible variation in the matching and the impedance bandwidth of the antenna. Figure 4 plots the surface

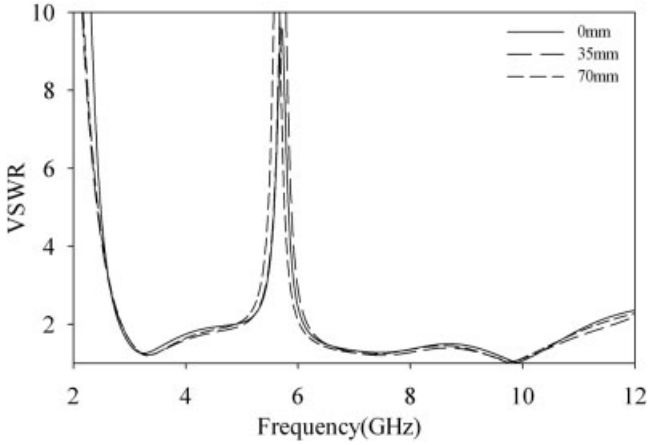

Figure 3 VSWR plot of the antenna for different ground lengths L'

current distribution on the antenna integrated with the PCB of a USB dongle. It is observed that the majority of the electric currents are concentrated around the slot with very little current on the rest of the ground plane. As a result, the performance of the antenna is insensitive to the system ground plane of the USB.

3. EXPERIMENTAL RESULTS AND DISCUSSIONS

3.1. Frequency Domain Measurements

The prototype of the proposed antenna was fabricated and measured using Rhode and Schwarz ZVB20 VNA. The measured VSWR of this antenna with and without the slot in the tuning stub is plotted in Figure 5 and is validated with the simulated results. The VSWR characteristics reveal UWB behavior with a 2:1 VSWR bandwidth from 2.9 to 11 GHz. When the slot is introduced in the tuning stub, a high VSWR (>4) occurs at around 5.5 GHz. In the pass band, the VSWR of the antenna is only slightly affected by the presence of the slot in the tuning stub.

The measured and simulated radiation patterns in the *X*-*Z*, *Y*-*Z*, and *X*-*Y* planes of the antenna for three different frequencies are shown in Figure 6. The patterns are stable throughout the band and resembles that of a monopole; omnidirectional in the H-plane (*X*-*Z*) and bidirectional in the E-planes (*Y*-*Z* and *X*-*Y*) throughout the band. Polarization of the antenna is along the *Y* direction. Measured peak gain of the antenna is compared with the simulated one in Figure 7 along with the radiation efficiency. The plots show reasonable agreement with a peak gain above 2 dBi throughout the band except at the notched frequency where it is as low as −13 dB

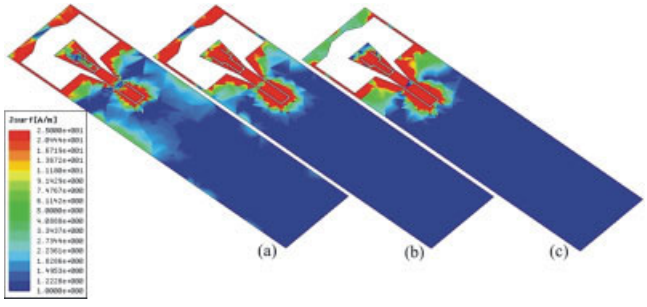

Figure 4 Current distribution on the antenna integrated with the PCB of a USB dongle (a) 3.3 GHz, (b) 6.5 GHz, and (c) 10 GHz. [Color figure can be viewed in the online issue, which is available at www.interscience.wiley.com]

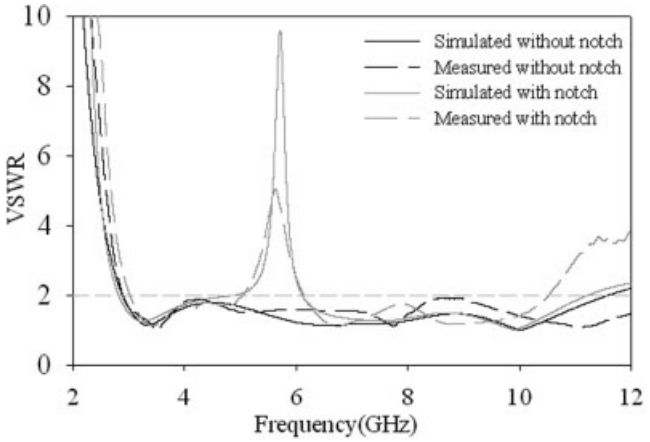

Figure 5 VSWR of the proposed antenna

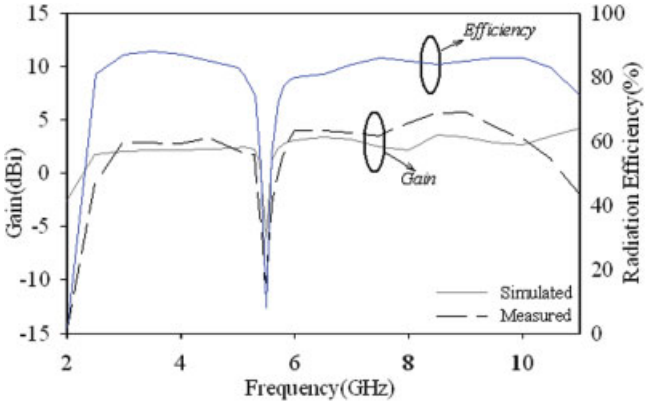

Figure 7 Gain and Radiation efficiency of the antenna. [Color figure can be viewed in the online issue, which is available at www.interscience.wiley.com]

when compared with the rest of the band while the radiation efficiency is more than 85% in the pass band.

3.2. Time Domain Measurement

Measurement of group delay is performed by exciting two identical prototypes of the antennas kept in the far field for two orientations; face-to-face and side-by-side. As shown in Figure 8(a), the group delay remains constant with variation less than a nanosecond for the face-to-face case, whereas the side-by-side orientation shows variation towards the higher frequency bands. In the presence of the notch characteristics, the group delay deteriorates at the notched frequency as shown in Figure 8(b).

The transmission coefficient, S_{21}, is measured in the frequency domain for the face-to-face and side-by-side orientations and is plotted in Figures 8(a) and 8(b). It shows fairly flat magnitude with

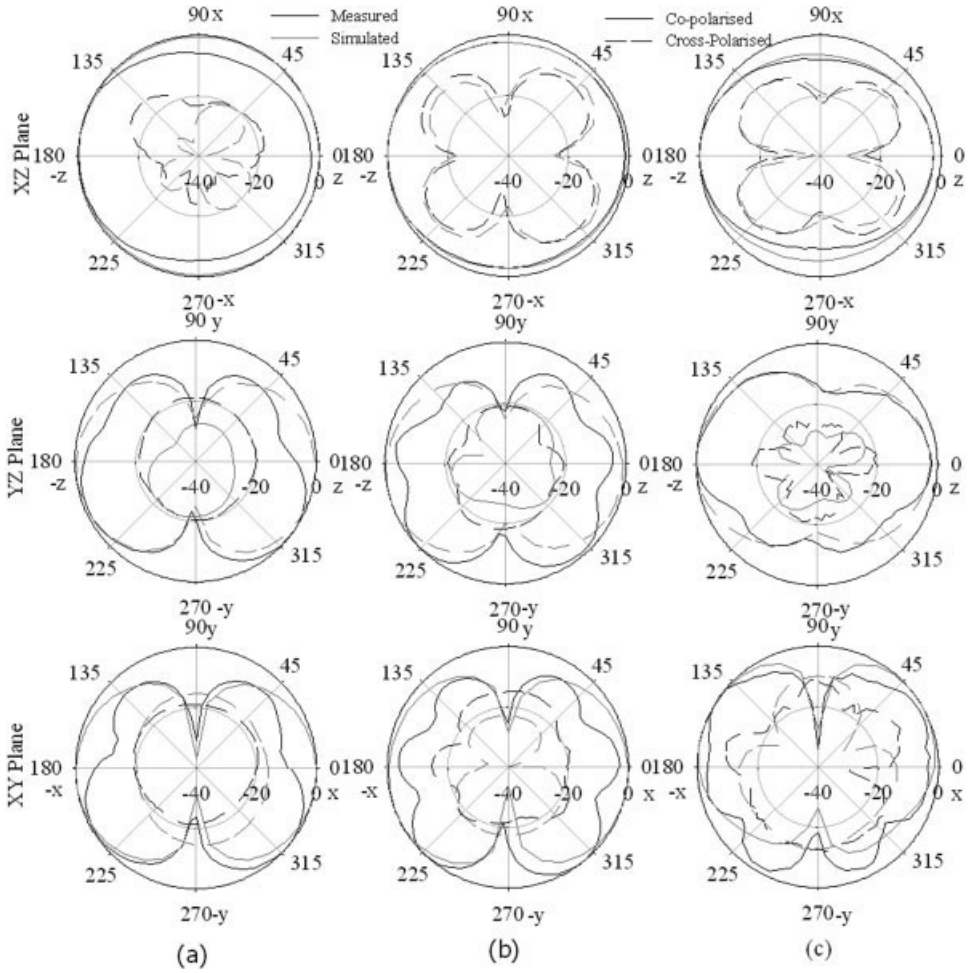

Figure 6 Radiation pattern of the antenna at (a) 3.35 GHz, (b) 6.5 GHz, and (c) 10 GHz

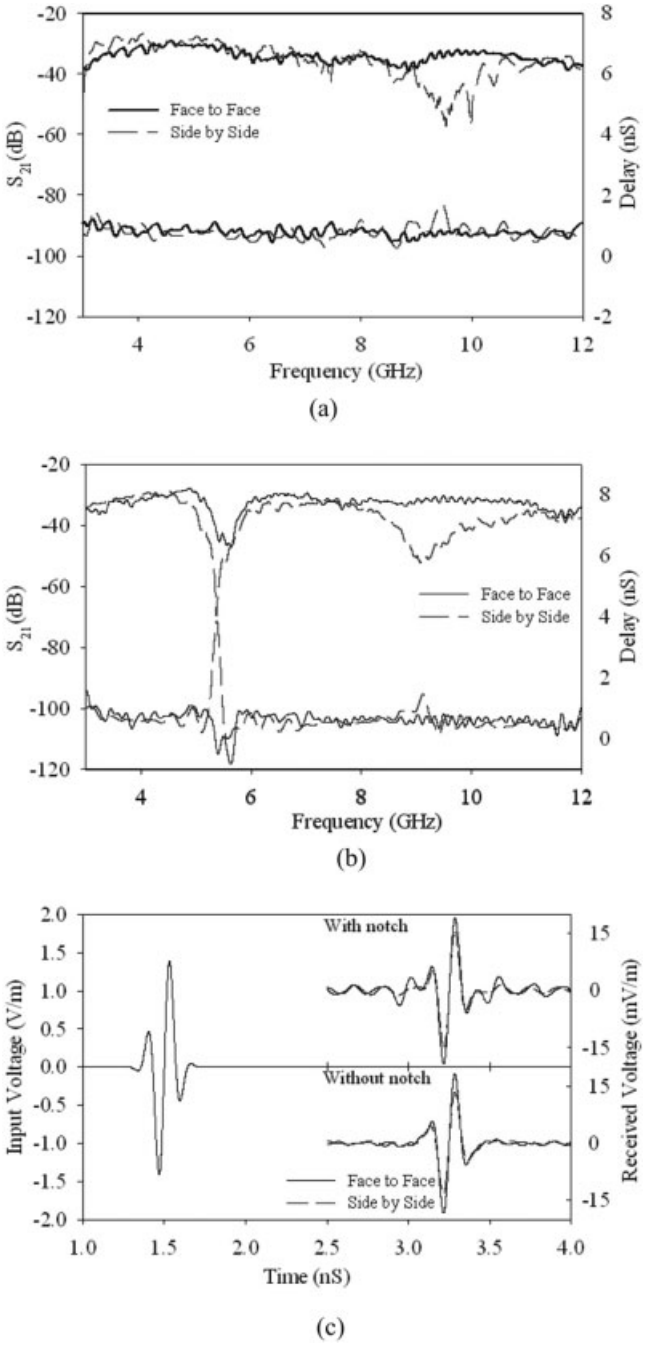

Figure 8 The measured group delay and S_{21} of the antenna (a) without notch characteristics and (b) with notch characteristics and (c) the input and recevied pulses

variation less than 10 dB throughout the band for both the orientations except at 9 GHz for the side-by-side case. This can be explained from the radiation pattern plotted in Figure 6(c) at 10 GHz where a drop in the radiated power is observed along the $\pm X$ direction when compared with that at its broadside (along Z axis). The transfer function is computed from this as in [13],

$$H(\omega) = \sqrt{\frac{2\pi R c S_{21}(\omega) e^{j\omega R/c}}{j\omega}} \tag{3}$$

where c is the free space velocity, and R is the distance between the two antennas. The transient response is obtained by convoluting a spectrum of incident pulse with the transfer function measured in the frequency domain.

The incident pulse chosen to be the a modulated Gaussian monocycle with mathematical form,

$$v_{\text{in}}(t) = A \sin(2\pi f_c t) e^{-(t/T)^2} \left(\frac{V}{m}\right) \tag{4}$$

This input pulse, plotted in Figure 8(c), is designed to fully cover the FCC band and comply with the emission standards specified when the amplitude constant $A = 1.61$. The pulse duration parameter T is chosen such that the pulse spectrum peaks at 6 GHz which in this case is 90 ps. The output waveform at the receiving antenna terminal is obtained as

$$s_o(t) = \Im^{-1}\{\Im\{s_i(t)\}H(\omega)\} \left(\frac{V}{m}\right) \tag{5}$$

The simulated output pulse with and without the notch characteristics for both face-to-face and side-by-side orientations of the antennas is shown in Figure 8(c). In both the figures, the side-by-side case is plotted with respect to the normalized face-to-face case. Although the maximum magnitude of the waveform for the side-by-side orientation is less than the face-to-face orientation, both the waveforms retain the information contained in the transmitted signal with minimum dispersion. The band notched designs exhibits slight ringing effect.

4. CONCLUSION

The design, fabrication, and testing of a compact UWB slot antenna fed by CPW with a band notch at 5.45 GHz is proposed. The impedance bandwidth of the designed antenna ranges from 2.64–10.9 GHz with a notched band at 5.45 GHz. The antenna features all the desirable characteristics demanded by UWB communication systems. It has adequate impedance bandwidth and stable radiation patterns throughout the ultra wide band and a good time domain performance. In addition to a compact size, the antenna is insensitive to the ground plane length variations making it suitable for wireless, universal, serial-bus (WUSB) dongle, and mobile UWB applications.

ACKNOWLEDGMENTS

Deepti Das Krishna and M. Gopikrishna acknowledge the Department of Science and Technology and the University Grants Commission, respectively, for providing financial assistance for the work. The measurements were carried out using the facilities created under DST-FIST program.

REFERENCES

1. http://www.intel.com/technology/comms/wusb/.
2. http://www.i2r.a-star.edu.sg/files/phatfile/tech_UWB.pdf.
3. Z.N. Chen and T.S.P. See, Small printed ultrawideband antenna with reduced ground plane effect, IEEE Trans Antennas Propag 55 (2007), 383–388.
4. S.-W. Su, J.-H. Chou, and K.-L. Wong, Internal ultrawideband monopole antenna for wireless USB dongle applications, IEEE Trans Antennas Propag 55 (2007), 1180–1183.
5. Federal Communications Commission, First Report and Order in the matter of Revision of Part 15 of the Commission's Rules Regarding Ultra-Wideband Transmission Systems, ET-Docket 98–153, 2002.
6. P. Li, J. Liang, and X. Chen, Study of printed elliptical/circular slot antennas for ultrawideband applications, IEEE Trans Antennas Propag 54 (2006), 1670–1675.
7. E.S. Angelopoulos, A.Z. Anastopoulos, D.I. Kaklamani, A.A Alexan-

dridis, F. Lazarakis, and K. Dangakis, Circular and elliptical CPW-Fed slot and microstrip-fed antennas for ultrawideband applications, IEEE Antennas Wireless Propag Lett 5 (2006), 294–297.
8. S.-W. Qu, J.-L. Li, J.-X. Chen, and Q. Xue, Ultrawideband strip-loaded circular slot antenna with improved radiation patterns, IEEE Trans Antennas Propag 55 (2007), 3348–3353.
9. Y.-C. Lin and K.-J. Hung, Compact ultrawideband rectangular aperture antenna and band-notched designs, IEEE Trans Antennas Propag 54 (2006), 3075–3081.
10. S. Cheng, P. Hallbjorner, and A. Rydberg, Printed slot planar inverted cone antenna for ultrawideband applications, IEEE Antennas Wireless Propag Lett 7 (2008), 18–21.
11. W.J. Lui, C.H. Cheng, and H.B. Zhu, Compact frequency notched ultra-wideband fractal printed slot antenna, IEEE Microwave Wireless Compon Lett 16 (2006), 224–227.
12. Ansoft, Ansoft HFSS v. 9.0, Ansoft Inc., Pittsburgh, USA.
13. W. Sorgel and W. Weisbeck, Influence of the antennas on the ultra-wideband transmission, EURASIP J Appl Signal Process 3 (2005), 296–305.

DESIGN OF A PROTECTIVE GARMENT GPS ANTENNA

L. Vallozzi,[1] W. Vandendriessche,[1] H. Rogier,[1] C. Hertleer,[2] and M. Scarpello[1]
[1] Department of Information Technology, Ghent University, Sint-Pietersnieuwstraat 41, 9000 Ghent, Belgium; Corresponding author: luigi.vallozzi@ugent.be
[2] Department of Textiles, Ghent University, Technologiepark Zwijnaarde 907, 9052 Zwijnaarde, Belgium

Received 23 September 2008

ABSTRACT: *A protective garment patch GPS antenna, for wearable textile systems applications, was designed and, for the first time in literature, realized in fire-resistant and water-repellent textile materials, making it particularly suitable for integration into rescue workers' garments. Measurements show that the antenna still performs adequately even when covered with protective textiles, and when integrated into a jacket, worn on the human body.* © 2009 Wiley Periodicals, Inc.
Microwave Opt Technol Lett 51: 1504–1508, 2009; Published online in Wiley InterScience (www.interscience.wiley.com). DOI 10.1002/mop.24372

Key words: *global positioning system; rescue workers' garments; textile antenna; wearable textile system*

1. INTRODUCTION

Nowadays wearable computing and wearable textile systems represent fast growing fields of application for garment patch antennas. In this context the global positioning system (GPS) plays an important role in real-time and continuous monitoring of position and speed of mobile users.

GPS antennas are usually realized with rigid materials and integrated into portable mobile equipment. Antennas made out of textile materials, including circularly polarized antennas suitable for GPS applications, were already introduced in [1–3], allowing easy integration into garments. Since rescue workers and especially firemen operate in harsh conditions, textile materials with special characteristics are needed. Up to now, water-repellent substrates have been already proposed as textile antenna substrate [4]. As improvement, we designed and realized a GPS antenna based on a fire-resistant and water-repellent foam substrate, yet flexible conductive textile materials that do not hinder the movements of the rescue worker. By using a truncated corner nearly square patch topology [5, 6], circular polarization is achieved.

Moreover, in real-work situations the antenna will be subjected to several effects which will alter the matching and the radiation characteristics with respect to the ideal situation in which the design has been carried out (i.e., with the antenna in planar state, in open space and with an infinitely wide ground plane). For this reason, several measurements were performed, resembling the real-work situation, to prove the performance robustness under these circumstances. In available literature the effects of the vicinity of the human body, on return loss and gain pattern, were investigated in [7] by means of simulations only. In contrast to these results, we measured the performances in terms of return loss, gain patterns, and axial ratio, when the antenna is covered by the textile layers composing a typical firemen jacket, and also when the antenna is integrated into a jacket, worn by a real human.

The article describes the results of these measurements and it is organized in the following way: in Section 2 the antenna topology and the design procedure are described; in Sections 3, 4, and 5 the results of the measurements of the three studied characteristics of the antenna are described, which are return loss, axial ratio as a function of the frequency, and gain patterns on the main planes of the antenna, respectively. Each one of the Sections 3, 4, and 5 is further divided into subsections, describing respectively the results in the three following situations: "antenna in open space," "antenna covered with additional textile layers," and "antenna integrated into a jacket, on human body." In Section 6, the conclusions are drawn.

2. ANTENNA TOPOLOGY AND DESIGN

Given the GPS-L1 standard, the design requirements are that, in the [1.56342, 1.58742] GHz frequency band, the return loss S_{11} remains lower than -10 dB and the axial ratio AR (defined as the ratio between the amplitudes of the orthogonal components composing the circularly polarized field) remains smaller than 3 dB. Therefore, an antenna topology was chosen consisting of a nearly square patch with two truncated corners, as shown in Figure 1. Right hand circular polarization was ensured by positioning the feed in the top right corner of the patch, as shown in Figure 1. The optimal antenna parameters, given the specifications for return loss and axial ratio in the frequency band of interest as optimization goals, are shown in Table 1. Finally, prototypes were realized by constructing the patch using FlecTron® or ShieldIt®, being electrotextiles with a sheet resistivity smaller than 0.1 Ω/sq, and the ground plane using FlecTron®. The substrate consists of a layer of fire-resistant and water-repellent closed-cell foam with a density of 187.3 kg/m^3, thickness $h = 3.94$ mm, and relative dielectric permittivity $\varepsilon_r = 1.56$.

3. RETURN LOSS MEASUREMENT AND SIMULATION

3.1. Antenna in Open Space

For several prototypes we measured the return loss using an HP8510C Network Analyzer, the antenna being placed in an anechoic chamber simulating open space. The measured S_{11}-curves for two prototypes are shown in Figure 2, together with the simulated one, obtained by means of the full-wave field simulator ADS-Momentum. One notices a measured -10 dB return loss bandwidth of 122 MHz ([1.530, 1.652] GHz) for the first prototype and 117.5 MHz ([1.5475, 1.665] GHz) for the second prototype, compared to a simulated bandwidth of 104 MHz ([1.532, 1.636] GHz) obtained by the design.